Journal of Solar Energy Research (JSER)

Journal homepage: jser.ut.ac.ir

Preparation of Hollow TiO_2 Nano-Spheres, ZnO and Fe_2O_3 in Sunscreens to Absorb Harmful Ultra Violet Rays

Fatemeh Naderi Bani[a], Mojtaba Goodarzi[a,*] and Davood Ghanbari[a]

[a]*Department of Science, Arak University of Technology, Arak 3818146763, Iran*

Received: 2020-10-05
Accepted: 2020-10-21

Abstract

For preparation of an effective sunscreens three nanoparticles were added to the matrix for suitable improving of sun absorption. In this study, different types of hollow TiO_2, ZnO, Fe_2O_3 were synthesized by sol-gel method. To prepare TiO_2 nanoparticles, tetra isopropoxide (TTIP) was used as a precursor and methanol as a solvent and its photocatalytic properties were investigated. Colorants and industrial wastewater were used to study photocatalytic properties of pure titanium dioxide, zinc oxide and iron oxide. The prepared products were characterized by X-ray diffraction (XRD), scanning electron microscopy (SEM), and Fourier transform infrared (FT-IR) spectroscopy and UV-vis absorption. All the synthesized products were used for preparation of sunscreen cream composite.

Keywords: Nanostructures, Nanocomposite, Hydrothermal, Photo-catalyst, Nanoparticles

Introduction

Today, many cosmetics for protecting sun ray combine UV filters are used while there is a few research to determine these compounds in sunscreens. There is no report to carbon-zinc oxide and carbon structures -Titanium dioxide indicates a reduction in the sun ray compared to pure titanium. Therefore, the use of these nano-composites in sunscreens creates a micro- layer, which gradually penetrates and protect skin against cancer. Investigation and study of structural, photocatalytic, optical, elemental and chemical properties of samples were evaluated using different methods such as XRD, SEM, FT-IR, UV-Vis, and the photocatalytic properties of nanocomposites prepared in the sunscreen cream. Therefore, the use of nanostructured composites in the sunscreen creates the most protection against ultraviolet radiation UVA-UVB. If titanium dioxide is combined with other blockers, like oxide, it is more beneficial for the skin and acts as a micro cover. In addition, porous iron oxide protects the skin from light waves and is a good supplement to limit UV rays [1-5]. Among different semiconductors, titanium dioxide (TiO2) and zinc oxide (ZnO) are the most popular photo catalysts that have demonstrated a high photosensitivity and chemical stability. They are non-toxic and low cost photo catalysts with stable photo generated electrons and holes under UV light irradiation. Among those

nanoparticles, titanium dioxide (TiO2) is frequently used in the production of paints, paper, plastics, welding rod-coating material, cosmetics, etc. Activated by UV-A irradiation, its photocatalytic properties have been utilized in various applications. Also it has applications like medical, environmental, sensor, photocatalytic and also its health impact for long-term exposure are discussed. Firstly, Titanium nanoparticles were synthesized by a (Tetra is prop oxide) TTIP chemical material, and hollow TiO_2 nanocomposites were prepared via a green Sol-Gel method. The photocatalytic behaviour of C-TiO_2 nanocomposite was evaluated using the degradation of acid black and acid blue and methyl orange under UV light irradiation [6-9].

ZnO nanoparticles were synthesized by a chemical precipitation, $Zn(NO_3)_2$ and then ZnO hollow nanoparticles nanocomposites were prepared via a green hydrothermal method in the presence of ammonia. Effects of time, pH and photo catalyst field on the morphology and particle size of the products were investigated. These nanoscale materials can generate highly oxidizing reactive oxygen species when exposed to ultraviolet radiation, the anatase phase of TiO_2 is more active than the rutile phase in photo catalysis [10-12]

2. Materials and Methods

2.1. Materials and methods

All the precursors and salts were purchased from Sigma-Aldrich or Merck company. Purity of the products were around 99.9 %. XRD patterns were recorded by a Philips, X-ray diffractometer using Ni-filtered CuKα radiation. SEM images were obtained using a KYKY-EM3200 instrument model 1455VP. All the chemicals were used as received without further purifications, Hollow carbon titanium dioxide show an increase in photo-catalyst's properties by increasing the surface to volume ratio with an average diameter of 58., SEM operating at 20 kV with a magnify output of 40 000X.

2.2. Synthesis of C/TiO_2 nanoparticles

First 0.36g of titanium tetraisopropoxide (TTIP) of were dissolved in 30 ml of distilled methanol, and then 0.11 g of nanocarbon was mixed on magnetic stirrer for 10 min. Then 1 ml of water distilled water and 2 ml HNO_3 solution as precipitator the pH of solution and was fixed to 2. The product then was dried in oven for 1h and was calculated at 500°C for 2h.

2.3. Synthesis C-ZnO nanoparticles hydrothermal method

0.3 g of carbon were dissolved in 200 ml of distilled water. 1 g of Zn $(NO_3)_2$ was then added to the solution, and it was mixed on magnetic stirrer for 10 min. Then 1/5ml of NH3 was slowly added as precipitator, until pH of the solution reach to pH: 9. The resultant solution was then transferred to a Teflon-lined stainless steel autoclave and was heated at 160 °C for 6 h. The obtained light yellow precipitate was washed twice with distilled water. The product then was dried in oven for 1h and was calcinated at 500°C for 2h.

2.4. Sunscreen synthesis contains ZnO, Fe2O3 and TiO2 nanocomposites

Firstly 1gr of synthesized hollow core ZnO was dispersed in 80 gr of cold cream made of (Vaseline, lanolin, paraffin, oyseren, glycerine, Distilled water, Wool oil) we do mix. Then 1gr of hollow core TiO_2 was added to the cream and was mixed for 10 min. After that 10ml of glycerine was slowly added to, Materials and we do mix for 10 min. After that 1g of PABA (Para amino benzoic acid) and 10 ml distilled water (ionized water) were added.

3. Results & Discussion

Fig. 1-a) illustrate schematic preparation of TiO_2 nanocomposite and hollow structures, also Fig. 1-b) show ZnO nanocomposite preparation schematically. Fig. 2-a) illustrates XRD pattern of carbon-titanium dioxide product. It can be observed that pure cubic phase of TiO_2 (JCPDS No.71 -1166, Space group: Anatase) is present in the pattern. Fig. 2-b) illustrates XRD pattern of Fe2O3 product JCPDS No.79 -0007, results confirm preparation of pure hematite phase of nanostructures without any major impurity. Fig. 2-c) illustrates XRD pattern of ZnO product. It can be observed that cubic phase of (JCPDS No 80-0074) is present in the pattern. Fig.

2-d) illustrates XRD pattern of cream composite product. It approves presence of all phases in the pattern.

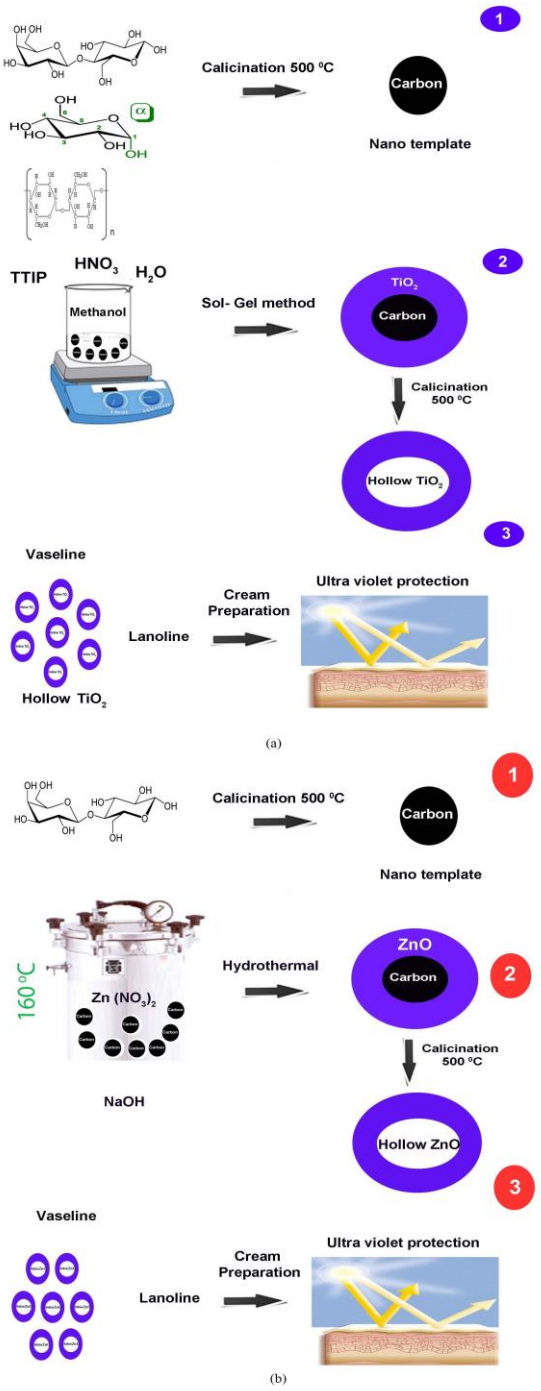

Fig.1 Schematic of preparation of a) hollow TiO_2 nano-structures and b) ZnO nanocomposite

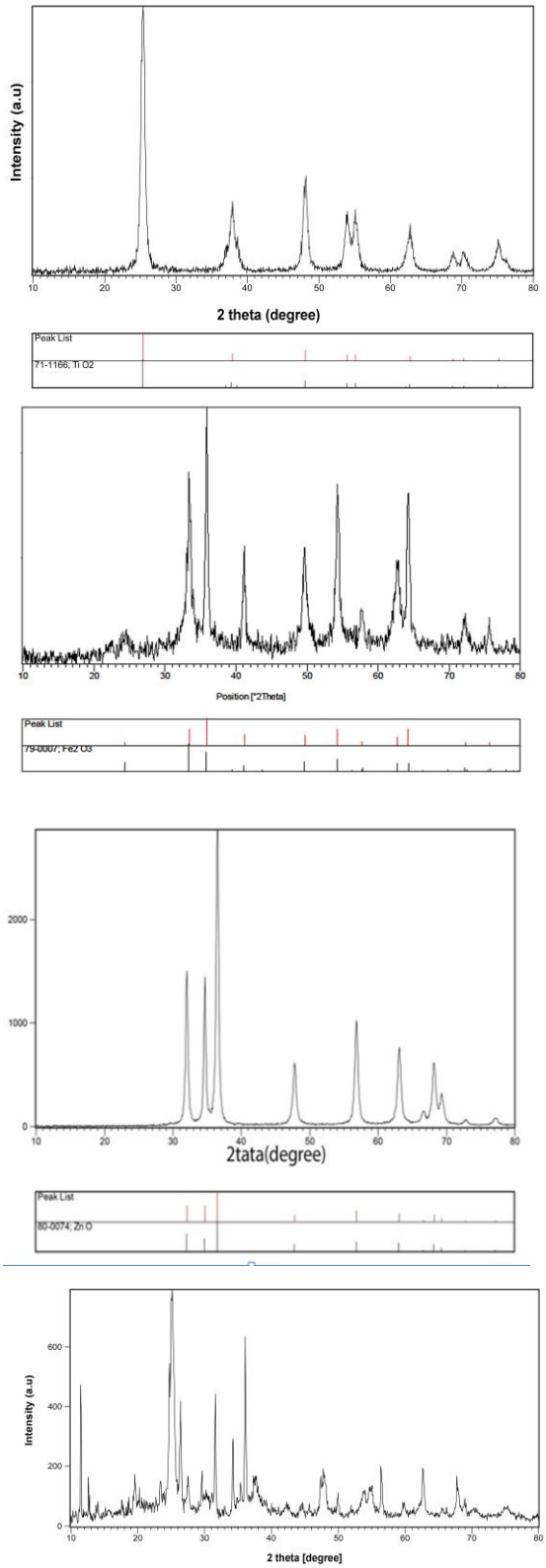

Fig 2 a) XRD patterns of C/TiO2, b) Fe_2O_3

nanoparticles, c) ZnO nanoparticles and d) XRD pattern of a Cream Composite

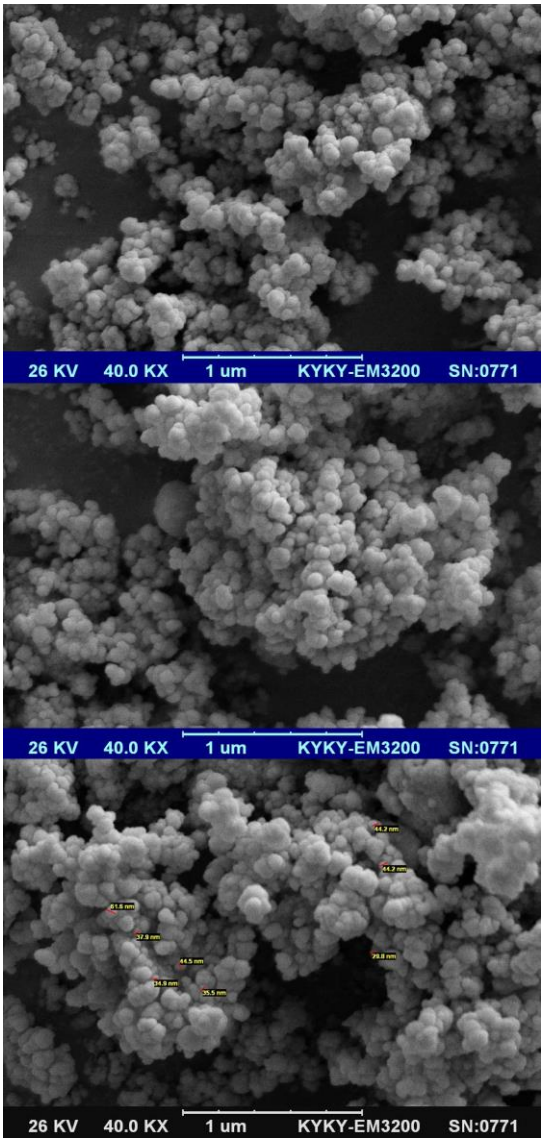

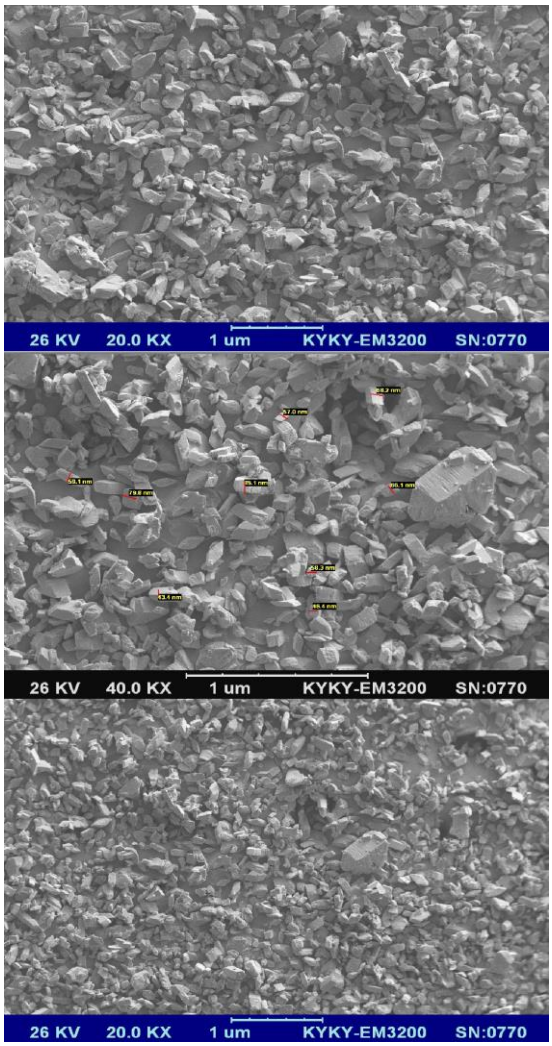

Fig. 3 SEM images of a) carbon nanoparticles prepared by lactose and b) carbon nanoparticles prepared by glucose

Figs. 3-a) illustrate SEM images of as-synthesized carbon from lactose nanoparticles in 2 h and 300 °C. The images indicate that the nanoparticles with average diameter size 41nm of less than 100 nm were prepared. Outcomes approve the nucleation was preferential compared to the crystal growth and lower sizes were obtained compare to other powders. Figs. 3-b) illustrate SEM images of as-synthesized carbon from glucose nanoparticles in 2 h and 300 °C. The images indicate that the nanoparticles with average diameter size (57) nm of less than 100 nm were prepared. Outcomes approve the nucleation was preferential

compare to the crystal growth and lower sizes were obtained compare to other powders.

Figs. 4-a_ illustrate SEM images of the TiO2 nanoparticles obtained at 2 h and 500 °C show perfect spheres nanoparticles with diameter size of about 54 nm. Figs. 4-b) show SEM images of the C/TiO_2 nanoparticles obtained at 2 h and 500 °C show perfect spheres nanoparticles with diameter size of about 58 nm. Figs. 5 depict various magnifications SEM images of the TiO_2 hollow spheres with potential of 10kV, obtained at 2 h and 500 °C show perfect spheres, Figs. 6 illustrate SEM images of the a) ZnO flower-like nanostructures were synthesized. and Fe_2O_3 nanostructures, nano-rods were synthesized.

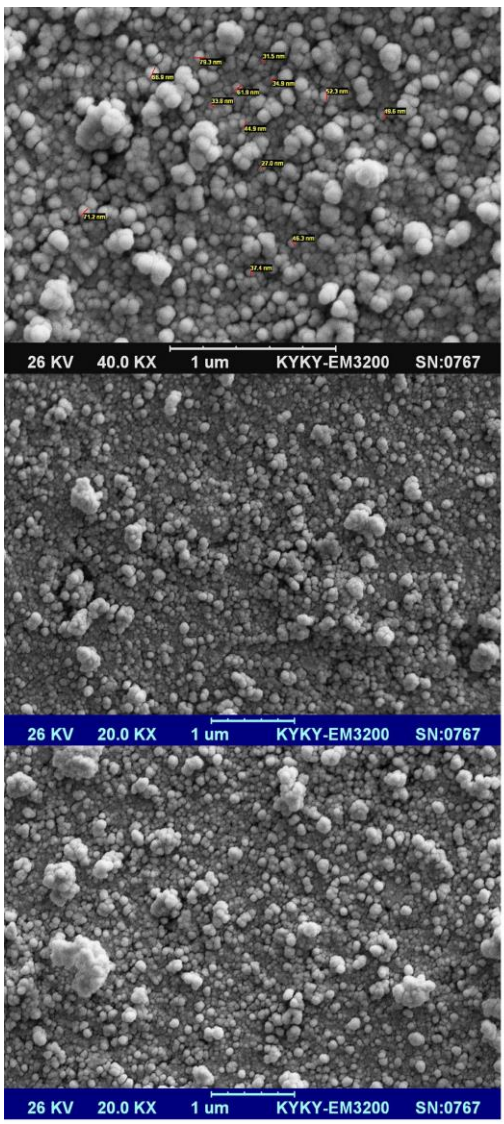

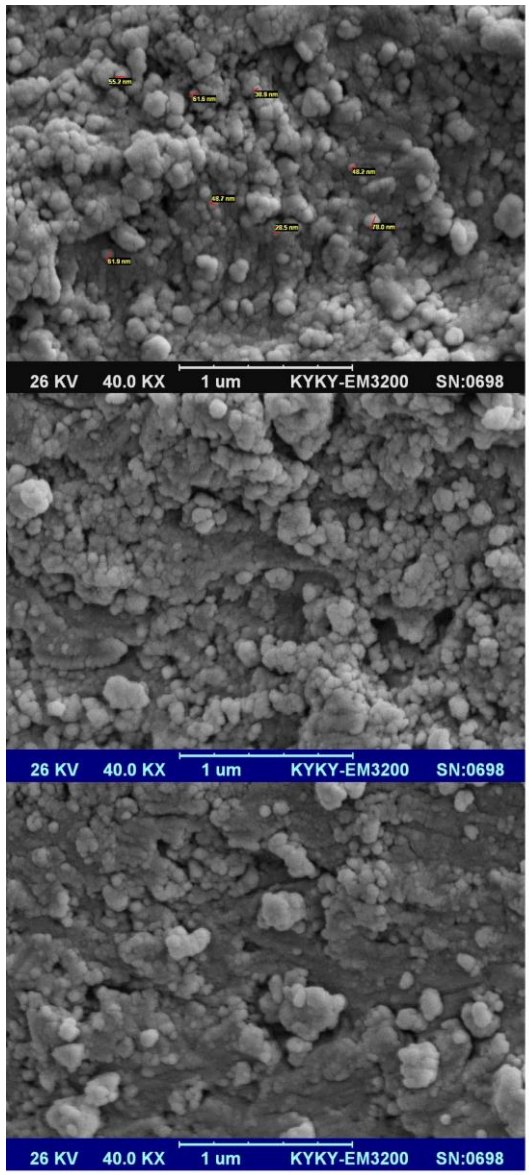

Fig. 4 SEM images of a) TiO_2 nanoparticles and b) C/TiO_2 nanocomposite

Figs. 7 shows the FT-IR spectrum of the as-prepared Fig.a) carbon from Lactose. The absorption bands at 588cm^{-1} are assigned to the titanium-oxygen (metal-oxygen bonds) stretching mode. The spectrum exhibits broad absorption a peak at 1421 and 1460 cm^{-1}, corresponding to the stretching mode of C - C group of adsorbed carbide group and a weak band near 3416 cm^{-1} which is assigned to O–H vibration mode due to the adsorption of moisture on the nanoparticles surface. (Fig. b) illustrate carbon

from glucose. The absorption bands at 734cm^{-1} are assigned to the Ti-O (metal-oxygen bonds) stretching mode. The spectrum exhibits broad absorption a peak at 1602 and 1714 cm^{-1}, corresponding to the stretching mode of C = O group of adsorbed Oxide group and a weak band near 3421 cm^{-1} which is assigned to bending vibration mode due to the adsorption of moisture on the nanoparticles surface. (Fig. c) is for titanium dioxide. The absorption bands at 588 cm^{-1} are assigned to the Ti-O (metal-oxygen bonds). stretching mode. The spectrum exhibits broad

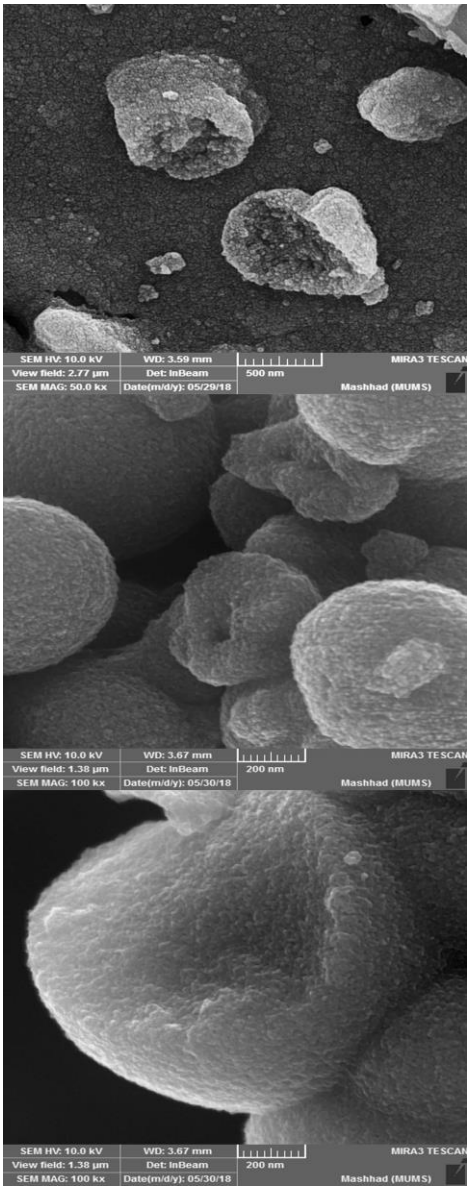

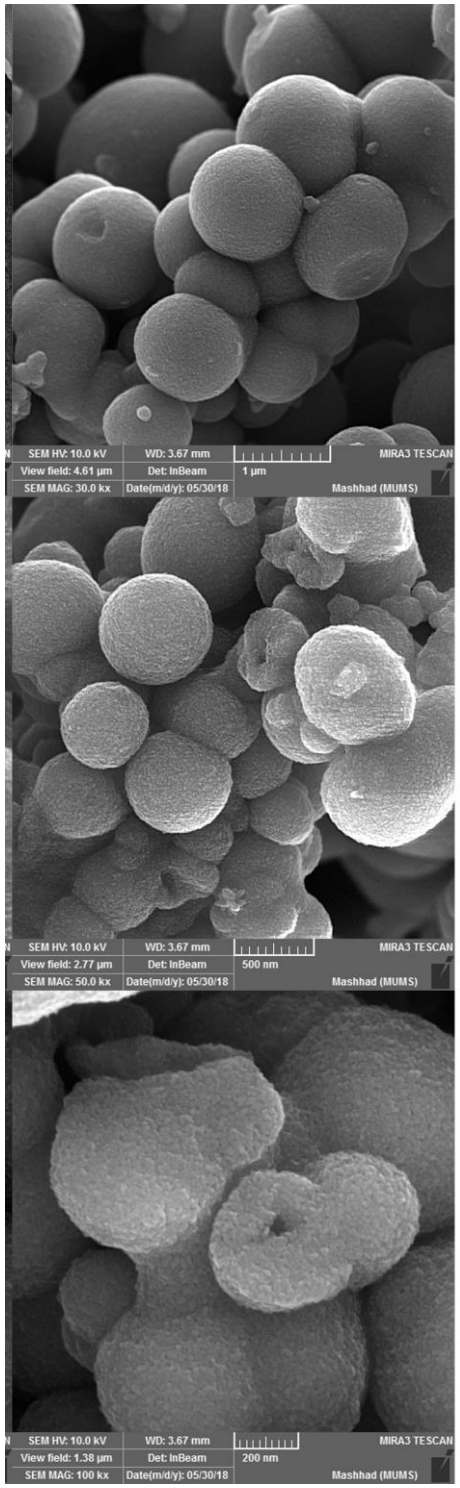

Fig. 5 SEM images of hollow nano spheres

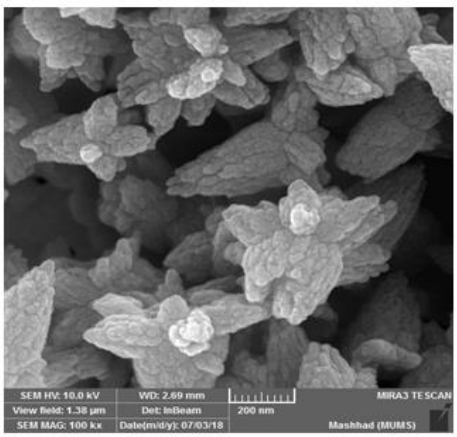

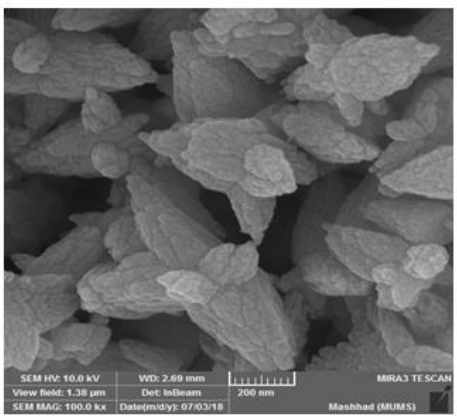

(a)

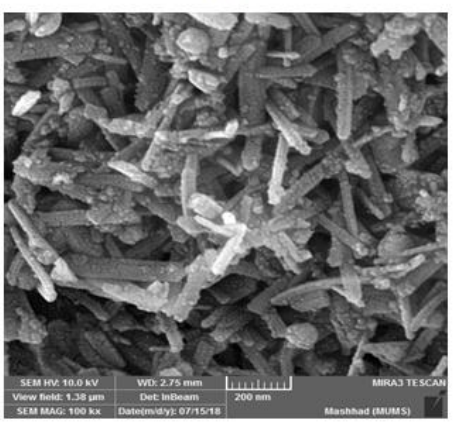

(b)

Fig. 6 SEM images of a) C/ZnO nano composite and b) C/Fe_2O_3 nano composite

absorption a peak at 1422 cm^{-1}, corresponding to the stretching mode of C=O group of adsorbed carboxyl group and a weak band near 3402cm^{-1} which is assigned to O–H bending vibration mode due to the adsorption of moisture on the nanoparticles surface. d) is spectrum of C-TiO_2 composite, The absorption bands at 501 cm^{-1} are assigned to the Ti-O (metal-oxygen bonds) stretching mode. The spectrum exhibits broad absorption a peak at 1630 cm^{-1}, corresponding to the stretching mode of C=O group of adsorbed carboxyl group and a weak band near 3402cm^{-1} which is assigned to O–H bending vibration mode due to the adsorption of moisture on the nanoparticles surface. e) is illustrate ZnO/TiO_2 cream composite. The absorption bands at 719 cm^{-1} are assigned to the Ti-O (metal-oxygen bonds) stretching mode. The spectrum exhibits broad absorption a peak at 1738 and 1643 cm^{-1}, corresponding to the stretching mode of C = O group of adsorbed carboxyl group and spectrum exhibits broad absorption a peak at 1169 and 1045 cm^{-1} corresponding to the stretching mode of C - O group of adsorbed carboxyl group and a weak band near 3361 cm^{-1} which is assigned to O–H bending vibration mode due to the adsorption of moisture on the nanoparticles surface.

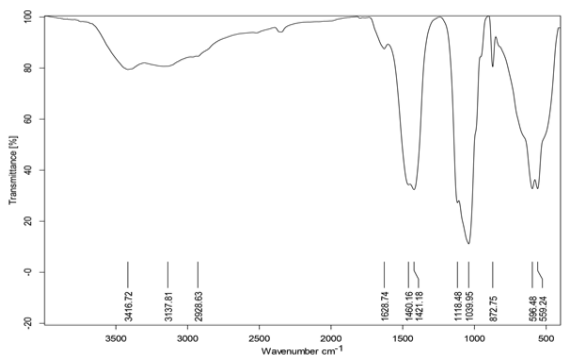

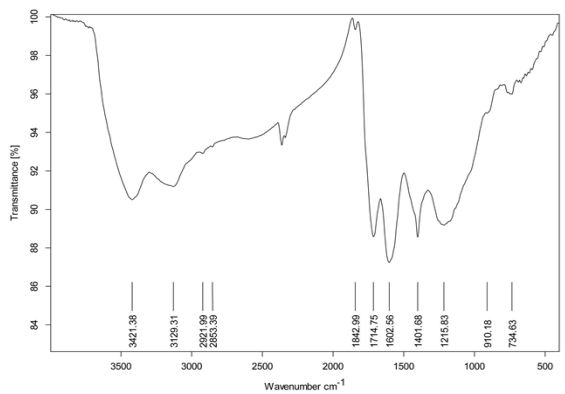

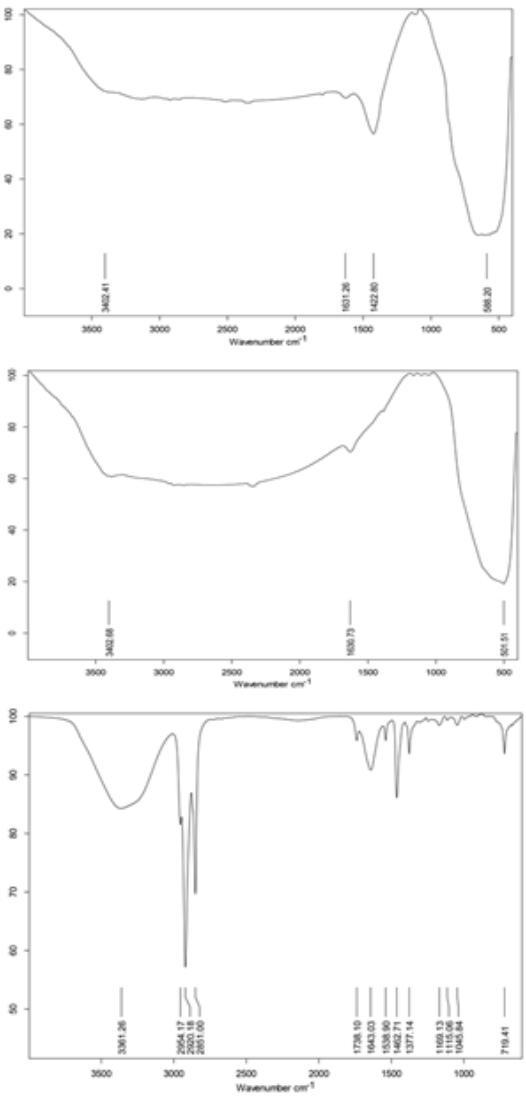

Fig 7. FT-IR spectrum of a) carbon nanoparticles by lactose, b) carbon nanoparticles by glucose, c) TiO_2 nanoparticles, d) C/TiO_2 hollow nanoparticles and e) cream composite

UV-Vis absorption spectra analysis

Photo-degradation in methyl orange and acid red through photocatalytic oxidation processes, which involve a large number of reactive types including h^+, O_2-, and OH radicals.

The photo–degradation of azo dye is shown in Fig. 8,

Following are the proposed reactions that occurred during the degradation of pollutants in the presence of TiO_2 :

$TiO2 + h\upsilon\ (UV) \rightarrow e^- + h^+$

$e- + O_2 \rightarrow O_2^-$

$h^+ + OH^- \rightarrow OH$

$O_2^- + H_2O \rightarrow OH$

OH + pollutants → degradation of pollutants [13-17].

The degradation ratio η(%) of dye was calculated by using the following equation:

$$\eta\ \% = = 100 \times [\ (A_0\text{-}A)\ ]/A_0 \quad (1)$$

Where A and A_0 are the absorbance of azo dye before and after exposure under simulated UV light, respectively..

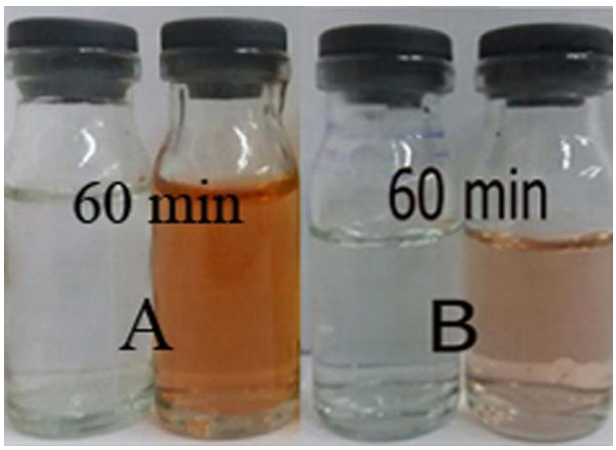

Fig 8. Photo-degradation under UV-vis irradiation (a) methyl orange (b) acid red

4. Conclusions

Different types of hollow TiO_2, ZnO, Fe_2O_3 were synthesized by sol-gel method. Titanium dioxide nanoparticles were prepared by tetra isopropoxide as a precursor and its photocatalytic properties were investigated. Colorants and industrial wastewater were used to study photocatalytic properties of pure titanium dioxide, zinc oxide and iron oxide. Phase of nanostructures were characterized by X-ray diffraction, shape and morphology was investigated by scanning electron microscopy, purity was examined by Fourier transform infrared spectroscopy and band gaps were estimated by UV-

vis absorption. All the synthesized products were used for preparation of sunscreen cream composite.

References

1. F. T. Tehama, E. Manikandan, MS. Dhlamini, M. Maaza. *Green synthesis of ZnO nanoparticles via Agathosma betulina natural extract. Mater Lett* 2015; **161** p 124 e7.
2. Y. Dan, H. Shi, C. Stephan, X. Liang. Rapid *analysis of titanium dioxide nanoparticles in sunscreens using single particle inductively coupled plasmaemass spectrometry. Microchem J* 2015; **122**: p 119-126.
3. K. Hedayati, M. Kord, M. Goodarzi, D Ghanbari, S Gharigh, *Photo-catalyst and magnetic nanocomposites: hydrothermal preparation of core–shell Fe_3O_4@PbS for photo-degradation of toxic dyes*, Journal of Materials Science: Materials in Electronics, 2017 **28** (2), p 1577-1589
4. P J Lu, et al, *Analysis of titanium dioxide and zinc oxide nanoparticles in cosmetics*, journal of food and drug analysis, 2015 **23** p 587 -594
5. P.J. Lu, S.W. Fang, W.L. Cheng, S.C. H *Characterization of titanium oxide and zinc oxide nanoparticles in sunscreen powder by comparing different measurement*, 26, 2018, p 1192-1200
6. A. N. Ossai, S. C. Ezike , A. B. Dikko, *Bio-synthesis of zinc oxide nanoparticles from bitter leaf (vernonia amygdalina) extract for dye-sensitized solar cell fabrication*, J. Mater. Environ. Sci., 2020 **11**, p 421-428
7. S. Hackenberg, et al, *Genotoxic effects of zinc oxide nanoparticles in nasal mucosa cells areantagonized by titanium dioxide nanoparticles*, Mutation Research, 2017 **816–817** p 32–37
8. F Kavousi, M Goodarzi, D Ghanbari, K Hedayati, *Synthesis and characterization of a magnetic polymer nanocomposite for the release of metoprolol and aspirin*, Journal of Molecular Structure, 2019 **1183**, p 324-330
9. A Naseri, M Goodarzi, D Ghanbari, *Green synthesis and characterization of magnetic and effective photocatalyst NiFe2O4–NiO nanocomposites*, Journal of Materials Science: Materials in Electronics, 2017 **28** (23), p 17635-17646
10. M Goodarzi, S Joukar, D Ghanbari, K Hedayati, *CaFe2O4–ZnO magnetic nanostructures: photo-degradation of toxic azo-dyes under UV irradiation*, Journal of Materials Science: Materials in Electronics, 2017 **28** (17), p 12823-12838
11. Z. A. Lewicka, W.W. Yu, B. L. Oliva, E. Q. Contreras, V.L. Colvin, *Photochemical behavior of nanoscale TiO2 and ZnO sunscreen ingredients, Journal of Photochemistry and Photobiology* A: Chemistry, 2013 **263** p 24– 33
12. G. Dransfield, P.J. Guest, P.L. Lyth, D.J. McGarvey, T.G. Truscott, *Photoactivity tests of TiO -based inorganic sunscreens*, Journal of Photochemistry and Photobiology B: Biology, 2000 **59** p 147–151.
13. K Hedayati, M Goodarzi, D Ghanbari, *Hydrothermal synthesis of Fe_3O_4 nanoparticles and flame resistance magnetic poly styrene nanocomposite*, Journal of Nanostructures, 2017 **7** (1), p 32-39
14. Y. Orooji, M. Ghanbari, O. Amirid and M. Salavati-Niasaric, *Facile fabrication of silver iodide/graphitic carbon nitride nanocomposites by notable photo-catalytic performance through sunlight and antimicrobial activity*, journal of Hazardous Materials,2020 **389**, p 122079
15. M. Ghanbari and M. Salavati-Niasari, *Tl_4CdI_6 Nanostructures: Facile Sonochemical Synthesis and Photocatalytic Activity for Removal of Organic Dyes*, Inorganic Chemistry2018 **57** p 11443–11455
16. S. Gholamrezaei, M. Ghanbari, O. Amiri, M. Salavati-Niasari, *Loke Kok Foong, $BaMnO_3$ nanostructures: Simple ultrasonic fabrication and novel catalytic agent toward oxygen evolution of water splitting reaction*, Ultrasonics Sonochemistry 2020 **61** p 104829
17. M. Ghanbari, F. Soofivand, M. Salavati-Niasari, *Simple synthesis and characterization of Ag_2CdI_4/AgI nanocomposite as an effective photocatalyst by co-precipitation method*, Journal of Molecular Liquids 2016 **223** p 21-28